HHS Public Access

Author manuscript

Oncogene. Author manuscript; available in PMC 2014 August 06.

Published in final edited form as:

Oncogene. 2014 February 6; 33(6): 679–689. doi:10.1038/onc.2012.636.

Upregulation of miRNA-155 promotes tumour angiogenesis by targeting VHL and is associated with poor prognosis and triple-negative breast cancer

W Kong[1,*], **L He**[1,*], **EJ Richards**[1], **S Challa**[1], **C-X Xu**[1], **J Permuth-Wey**[2], **JM Lancaster**[3], **D Coppola**[4], **TA Sellers**[2], **JY Djeu**[5], and **JQ Cheng**[1]

[1]Department of Molecular Oncology, H. Lee Moffitt Cancer Center and Research Institute, Tampa, Florida 33612, USA

[2]Department of Cancer Epidemiology, H. Lee Moffitt Cancer Center and Research Institute, Tampa, Florida 33612, USA

[3]Department of Women's Oncology, H. Lee Moffitt Cancer Center and Research Institute, Tampa, Florida 33612, USA

[4]Department of Pathology, H. Lee Moffitt Cancer Center and Research Institute, Tampa, Florida 33612, USA

[5]Department of Immunology, H. Lee Moffitt Cancer Center and Research Institute, Tampa, Florida 33612, USA

Abstract

MicroRNA-155 (miR-155) is frequently up-regulated in various types of human cancer; however, its role in cancer angiogenesis remains unknown. Here, we demonstrate the role of miR-155 in angiogenesis through targeting von Hippel-Lindau tumour suppressor (VHL) in breast cancer. Ectopic expression of miR-155 induced whereas knockdown of miR-155 inhibited HUVEC network formation, proliferation, invasion, and migration. Furthermore, mammary fat pad xenotransplantation of ectopically expressed miR-155 resulted in extensive angiogenesis, proliferation, tumour necrosis, and recruitment of pro-inflammatory cells such as tumour associated macrophages. Expression of VHL abrogated these miR-155 effects. Moreover, miR-155 expression inversely correlates with VHL expression level and is associated with late stage, lymph node metastasis, and poor prognosis as well as triple-negative tumour in breast cancer. These findings indicate that miR-155 plays a pivotal role in tumour angiogenesis by downregulation of VHL, and provide a basis for miR-155-expressing tumours to embody an aggressive malignant phenotype, and therefore, miR-155 is an important therapeutic target in breast cancer.

Correspondence to: JQ Cheng, PhD, MD, Departments of Molecular Oncology, H. Lee Moffitt cancer Center and Research Institute, 12909 Magnolia Dr., SRB3, Tampa, FL 33612. Jin.Cheng@moffitt.org.

*Authors contributed equally to this work.

CONFLICT OF INTEREST

The authors declare no conflict of interest.

Keywords

miR-155; angiogenesis; VHL; breast cancer; inflammation

INTRODUCTION

Angiogenesis plays a major role in tumour growth, progression, and metastasis. Initially, angiogenic activity is absent in early neoplasms. However, as tumours progress, oxygen becomes depleted within the core which creates hypoxic conditions that induce HIFα family proteins through degradation of the von Hippel Lindau (VHL) tumour suppressor and production of angiogenic factors, including vascular endothelial growth factor (VEGF), fibroblast growth factor (FGF), platelet-derived growth factor (PDGF), epidermal growth factor (EGF), placental growth factor (PIGF), and angiopoietins-1 (ANG1) [1–6]. Tumour production of these factors promotes recruitment of endothelial precursor cells from the bone marrow, and vascular permeability factors such as VEGF allow these cells to penetrate vessel walls and migrate from a vessel in close proximity to the tumour towards the core of the tumour where these angiogenic stimuli are produced. Cells attach to pre-existing vessels and one another during proliferation to form tubular sprouts in pushing the circulatory network deeper into the tumour [2, 7–9]. The delivery of blood supply, via newly generated blood vessels, into the center of the tumour allows for continued tumour growth [10, 11].

MiRNAs are processed short single stranded RNA that forms a ribonucleoprotein complex with Argonaute proteins to inhibit gene expression [12]. While a number of miRNAs are deregulated in human cancer, only a few miRNAs have been reported to regulate tumour angiogenesis. For example, miR-107 and miR-591 suppress tumour angiogenesis, tumour growth and the expression of VEGF by inhibition of HIF1β and HIF-1α, respectively [13, 14]. MiR-93-expressing U87 glioma cells induce tumour blood vessel formation and tumour growth by integrin-β8 [15].

Accumulating studies show frequent upregulation of miR-155 in various human malignancies, including breast, lung, pancreatic and colon cancers as well as B cell lymphoma and chronic lymphocytic leukemia [16–20]. We and others previously demonstrated that miR-155 regulates a number of cell processes including cell survival, growth, migration, invasion, epithelial to mesenchymal transition (EMT) and immune response [21–29], yet the role of miR-155 in tumour angiogenesis remains elusive. In the current study, we provide *in vitro* and *in vivo* evidence that miR-155 promotes breast cancer angiogenesis by targeting VHL and the upregulation of miR155 is associated with metastasis, poor prognosis and triple-negative tumour in breast cancer.

RESULTS

miR-155 promotes angiogenesis

We initially observed that VEGF induced miR-155 expression (Figure 1a). To investigate the role of miR-155 in angiogenesis, we ectopically expressed and knocked down miR-155 in human umbilical vein endothelial cells (HUVEC) in the absence and presence of VEGF,

respectively (Figures 1b and 1c). HUVEC expressing miR-155 increased network formation, as measured by branch points and total tube lengths (top panels of Figure 1d). In agreement with previous finding [30, 31], VEGF treatment induced *in vitro* angiogenesis; however, knockdown of miR-155 decreased VEGF-induced network formation (bottom panels of Figure 1d). Since angiogenesis requires endothelial cell proliferation, migration and invasion [32, 33], we investigated the effect of miR-155 on these aspects by performing BrdU incorporation, and Boyden Chamber assays with (invasion) and without (migration) Matrigel, respectively. Ectopic miR-155 expression increased, whereas knockdown of miR-155 decreased BrdU incorporation compared to control (Figure 1e). Similarly, ectopic expression of miR-155 increased, whereas its inhibition decreased invasion and migration of HUVEC (Figures 1f and 1g).

To analyze the effect of miR-155 on breast cancer angiogenesis *in vivo*, we infected BT474 cells, which express low level of endogenous miR-155, with lentiviral pMIRNA-155 (BT474/miR-155) and empty vector as control (BT474/ctrl) (Figure 2a). It was noted that the level of miR-155 in BT474/miR-155 cells was comparable to, even slight lower than, endogenous miR-155 in HS578T and MDA-MB-157 cells (Figure S1). Stable BT474/miR-155 and BT474/ctrl cells were xenotransplanted into the right and left mammary fat pad of nude mice, respectively. The tumors from BT474/miR-155 and the control cells were monitored by IVIS Imaging system on day 5 (top of Figure 2b) and week 6 (bottom of Figure 2b) of the transplantation. Figure 2c shows BT474/miR-155 tumours grew at faster rate compared to BT474/ctrl. The average BT474/miR-155 tumour weight was approximately two times heavier than controls (Figure 2d). Blood vessels were apparent on the surface of BT474/miR-155 tumours, whereas control tumours had smaller and less defined blood vessels (Figure 2e). We next examined the expression of a panel of angiogenic factors in these tumours. Immunoblot analysis revealed that HIF1α, HIF2α and VEGF levels were elevated in BT474/miR-155 tumours compared to controls (Figure 2f).

In addition, a significant increase in neoangiogenic blood vessels and proliferation as well as mitotic index was observed in BT474/miR-155 tumour when compared to BT474/ctrl (Figures 2g and 2h; Supplementary Figure S2). Furthermore, immunofluorescence staining with antibodies against F4/80 and CD31 revealed macrophage infiltration in BT474/miR-155 tumours that was largely undetectable in control tumours (Figure 2i). Expression of miR-155 in these tumours was confirmed by qRT-PCR (Figure 2f). Taken collectively, these data indicate miR-155 plays a pivotal role in tumour angiogenesis.

MiR-155 down-regulates VHL and is associated with clinical features

With the observation of miR-155 inducing *in vitro* and *in vivo* angiogenesis, we next determined the underlying mechanism. Since increase of VEGF, HIF1α and HIF2α protein levels was observed in BT474/miR-155 tumours (Figure 2f), we initially examined the mRNA levels of VEGF, HIF1α and HIF2α in miR-155-transfected BT474 cell and its xenograft tumour. Real-time PCR analysis showed that HIF1α and HIF2α mRNA levels did not change while VEGF was considerably elevated in BT474/miR-155 tumours (Supplementary Figure S3). Because VHL is an E3 ligase of HIF1α and HIF2α [34], we next assessed if miR-155 regulates VHL level. Western blot analysis revealed that ectopic

expression of miR-155 in BT474 and HUVEC cells reduced VHL protein expression but not its mRNA level (Figure 3a). Accordingly, the expression of HIF1α, HIF2α and VEGF was increased in miR-155-transfected cells (Supplementary Figure S4). Furthermore, knockdown of miR-155 in HS578T and MDA-MB-157 cells, in which endogenous miR-155 is high, increased VHL expression (Figure 3b). Expression of VHL was also decreased in BT474/miR-155 xenograft tumours compared to BT474/vector controls (Figure 3c; Supplementary Figure S5). In addition, inverse correlation of expression of miR-155 and VHL was observed in a panel of breast cancer cell lines (Figure 3d). We also examined 231 breast cancer specimens for VHL and miR-155 levels by qRT-PCR/Western blot for frozen tissues or LNA-ISH/IHC for paraffin embedded tissues (Figures 3e; Supplementary Figure S6). Of the 231 breast tumours, 122 had elevated miR-155 and 125 had low levels of VHL. Of the 125 tumours with down-regulated VHL, 81 (66%) also had elevated miR-155 ($p < 0.042$; Figure 3f). These data suggest miR-155 down-regulation of VHL *in vitro* and *in vivo*.

Furthermore, we examined if miR-155 levels are related to clinical feature of breast cancer. Table 1 shows that elevated miR-155 is significantly associated with late stage (stage III/IV) and high grade tumours, lymph node metastasis and triple-negative breast cancer. Kaplan-Meier analysis of all 231 patients demonstrated a statistically significant negative correlation between overall survival (OS) and miR-155 expression level ($P<0.001$; Figure 4a). To extend this observation, we separated the patients into two groups by stage [e.g., late stages (III/IV) and early stages (I/II)] and asked whether within each subgroup miR-155 expression predicts patient survival. In both groups, high miR-155 expression was still a prognostic factor (Figures 4b and 4c). In addition, the patients whose tumours express high levels of miR-155/low levels of VHL exhibit even worse prognosis (Figure 4d vs. Figure 4b). These findings suggest that miR-155 regulates VHL resulting in a more aggressive phenotype in breast cancer.

Further univariate analysis revealed that several factors, including stage, histology and miR-155 expression were associated with poor clinical outcome ($P < 0.05$; Table 2). Of them miR-155 expression was a relative strong predictor of poor OS with a hazard ratio of 2.408 (95% CI, 1.491–3.888, $P<0.001$). A multivariate Cox proportional hazards model with following variables: age, stage, grade, histology and miR-155 expression, was used to analyze their simultaneous association with OS. While tumour stage was a strong independent predictor of outcome ($P=0.003$), miR-155 expression appeared to be even better independent predictor ($P<0.001$). These results indicate that miR-155 is a prognostic marker in breast cancer.

Identification of VHL as a direct target of miR-155

To determine if miR-155 directly regulates VHL, we initially searched pre-compiled databases but did not identify any canonical miR-155 binding sites within VHL-3'UTR region. We next performed AGO2 RNA immunoprecipitation in attempt to identify direct interaction between miR-155/AGO/RISC complex with mRNA of VHL (Figure 5a). Co-transfection of pre-miR-155 or pre-miR-control with Myc-AGO2 followed by anti-Myc immunoprecipitation and RNA isolation yielded RNA where qRT-PCR showed VHL mRNA enrichment in miR-155/AGO/RISC complex compared to control/AGO/RISC

complex (Figure 5b). However, the same isolated RNA revealed no significant enrichment in HIF2α or VEGF mRNAs in miR-155/AGO/RISC compared to control/AGO/RISC complex (Figure 5b). These findings suggest direct interaction between VHL mRNA and miR-155/AGO/RISC complex that prompted us to carry out further sequence analysis. Using RNA22 database, we found an atypical motif in VHL-3'UTR that partially matches the miR-155 “seed” sequence (Figure 5c).

To determine if this motif is responsible for down-regulation of VHL by miR-155, we cloned the VHL-3'UTR (i.e., 66-bp containing putative miR-155 response element) into the pMIR-REPORT luciferase vector (VHL-WT 3’UTR). In parallel, a mutated seed site in VHL-3'UTR was also cloned into the pMIR-REPORT vector (VHL-MUT 3’UTR). Transfection of VHL-WT 3’UTR into a panel of breast cancer cell lines showed the luciferase levels inversely correlated with endogenous miR-155 expression (Figure 5d). Co-transfection of miR-155 and VHL-WT 3’UTR into BT474 resulted in approximately 30% decrease in luciferase activity whereas no significant change was detected in the VHL-MUT 3’UTR transfection (Figure 5e). Further, inhibition of miR-155 in HS578T, a cell line with high endogenous miR-155, and co-transfection with VHL-WT 3’UTR resulted in almost 60% increased luciferase activity whereas no change was observed in the cells transfected with VHL-MUT 3’UTR (Figure 5f). Since miR-155 targeting sequence is located at very end of VHL-3’UTR, we also created 2 pMIR-REPORT constructs, one of which was 0.8-kb VHL-3’UTR containing miR-155 response element (MRE) and the other was a truncated deletion of miR-155 MRE sequence (VHL-3'UTR-0.68, Figure S7A). Luciferase assays revealed that miR-155 repressed the activity of pMIR-REPORT-VHL-3'UTR-0.8 but not pMIREPORT-VHL-3'UTR-0.68 (Figure S7B). These data indicate that the VHL is a direct target gene of miR-155.

Expression of VHL rescues miR-155-induced angiogenesis *in vitro* and *in vivo*

Having demonstrated miR-155 induces *in vitro* and *in vivo* angiogenesis and inhibits VHL expression, we proceeded to determine if miR-155 promotes angiogenesis through downregulation of VHL. We introduced HA-tagged VHL cDNA expression vector without the 3’UTR, which can escape miR-155 regulation, together with pre-miR-155 into HUVEC (Figure 6a). Notably, expression of VHL largely abrogated the effects of miR-155 on HUVEC endothelial network formation, BrdU incorporation, invasion and migration (Figures 6b–e).

We further evaluated the effect of ectopic expression of VHL on miR-155-induced angiogenesis in orthotopic breast cancer model. Lentiviral pMIRNA-155 stably infected BT474 BT474 cells (Figure 2a) were transfected with pcDNA-HA-VHL or pcDNA (Figure 7a). After injection of the cells into mammary fat pat of nude mice, the animals were examined for tumour growth for 6 weeks. As shown in Figures 7b and 7c, miR-155-induced tumour growth and tumour weight were significantly suppressed by VHL reintroduction. Furthermore, VHL restoration inhibited blood vessels, tumour associated macrophage infiltration and proliferation induced by miR-155 (Figures 7d–f). These results indicate that miR-155 promotes breast cancer growth and angiogenesis primarily by targeting VHL.

DISCUSSION

We and others previously demonstrated that miR-155 is frequently upregulated in human breast cancer [17, 19, 23, 35]. Previous studies have shown that miR-155 is induced by hypoxia and VEGF through HIFs [30, 31] and possible c-Myc or E2F [36], respectively. However, its role in angiogenesis remains underexplored. In this report, we demonstrate that miR-155 induces tumour angiogenesis and promotes breast tumour growth by targeting VHL (Figures 2, 5–7). Our findings show that VHL is down-regulated by miR-155 through direct interaction with a site within the 3'UTR of VHL. Although the VHL gene is frequently inactivated or silenced in clear cell renal carcinomas, haemangioblastomas, and pheochromocytomas through germline and/or somatic mutations or promoter hypermethylation, loss of VHL in breast cancer is not attributed to these anomalies [37, 38]. Our findings suggest that VHL loss in breast cancer can be partly attributed to miR-155 overexpression.

A well characterized function of VHL is targeting of the HIFα family members (HIF1, 2, and 3α) for proteolytic degradation, thus preventing dimerization with their respective β subunits in forming the functional transcriptional factor. Evidence suggests that HIF2α is the main downstream VHL target to play a causal role in VHL–/– renal carcinogenesis [34]. Under normoxic conditions where oxygen is present, members of the prolyl hydroxylase family (PHDs) enzymatically hydroxylates prolyl residues within the HIFα subunit to form high affinity binding sites for VHL. VHL, an E3 ubiquitin ligase, promotes rapid degradation of HIFα subunit. Conversely, as oxygen depletes during hypoxia, PHDs do not hydroxylate HIFα subunits, which then stabilize and dimerize with the HIFβ subunit in forming the functional transcriptional factor. In this report, we observed miR-155 down regulates VHL expression, resulting in HIF2α and HIF1α stability both *in vitro* and *in vivo* (Figures 2f and 3c). Accumulating studies have demonstrated that HIF1α and HIF2α promoted tumour angiogenesis, tumour invasion and triple- negative breast cancer phenotype by regulating a number of target genes including IL6, VEGFA, CD44, and PKM2 etc [39, 40]. Notably, a recent report showed that inhibition of HIF1α and HIF2α by SHARP1 repressed triple-negative breast cancer aggressiveness [41]. These findings suggest that miR-155 regulates VHL/HIF pathway to induce tumour angiogenesis and metastasis. This notion is further supported by the data that transfection of VHL cDNA without 3'UTR rescued miR-155-induced angiogenesis (Figures 6 and 7). We also noted a consequential increase in VEGF (Figures 2f and 3c), which likely contributes to the observed increase angiogenic activity both in HUVECs and breast cancer xenografts.

In addition, VHL also exhibits HIF-independent functions that include regulation of apoptosis and cell senescence. VHL also plays a role in microtubule stabilization, maintenance of the primary cilium, regulation of extracellular matrix formation, and cell to cell adhesion [42]. Although we have identified the proangiogenic activity of miR-155 through downregulation of VHL, whether miR-155 subverts these VHL mediated physiological processes for promoting malignancy remains to be investigated.

An angiogenic tumour is associated with microenvironments and immune cells that facilitate tumour progression and malignancy [43–45]. The endothelium of tumour blood vessels provides a physical structure for circulating immune cells derived from the bone marrow to

adhere, while angiogenic stimuli promotes chemotaxis, migration, and infiltration of these cells into the tumour. They include macrophages, neutrophils, mast cells, and Myeloid-derived suppressor cells (MDSCs) [7, 8, 9, 46]. In agreement with this, we observed infiltration of tumour associated macrophages (TAMs) in miR-155 tumours that was largely absent in control tumours (Figures 2i and 7f). In future studies, cytokine analysis could provide further insights on the role of miR-155 in tumour inflammation, leading to tumour progression. For instance, tumour production of IL-4 activates tumour-associated macrophages (TAMs), which in turn produce matrix-degrading enzymes to promote tumour invasion. TAMs can also produce proangiogenic and miR-155 inducing factors such as VEGF, IL-1, bFGF, and TNFα, to initiate a vicious feed forward cycle between tumour angiogenesis and inflammation [24, 27, 31, 47, 48] (Figure 8).

In agreement with miR-155 induction of angiogenesis, we also show that up-regulation of miR-155 is associated with metastasis, late stage/high grade tumour and poor prognosis in breast cancer. Moreover, its prognosis value is independent of tumour stage (Fig. 4). In addition, we found elevated level of miR-155 in a significant portion of triple-negative breast cancer (Table 1). A recent study demonstrated that up-regulation of miR-155 in BRCA1 deficient or BRCA1 mutant human breast tumours and that BRCA1 epigenetically represses miR-155 expression by recruiting HDAC2 complex to the miR-155 promoter [49]. Previous reports showed that downregulation/mutation of BRCA1/2 is associated with triple-negative breast cancer [50, 51]. While the role of miR-155 in triple negative breast cancer is current unknown, these findings suggest that miR-155 could be a valuable marker and target of this subgroup tumour.

Our findings are important for several reasons. We show miR-155 directly down regulates VHL which provides another mechanism for VHL loss in breast cancer in addition to mutations and promoter hypermethylation. We also present for the first time, the role of miR-155 in tumour angiogenesis that contributed to increased progression of breast tumours. Moreover, miR-155 could be an independent prognostic marker of breast cancer and plays a role in triple negative tumour. Taken together with our earlier reports that link miR-155 with breast cancer chemoresistance and mammary EMT, invasion and migration [22, 23], miR-155 is a critical therapeutic target in breast cancer.

MATERIALS AND METHODS

Reagents and antibodies

TRIZOL®, Pre-miR™ miRNA and Taqman® Pri-miRNA kit were purchased from Life Technologies Corporation (Carlsbad, CA). 5-Bromo-2'-deoxy-uridine Labeling and Detection Kit I was purchased from Roche Applied Sciences (Indianapolis, IN). Anti-VHL rabbit polyclonal antibody was purchased from Cell Signaling Technology (Danvers, MA). Antibodies against Myc and VEGF were from Santa Cruz Biotechnology (Santa Cruz, CA). Anti-CD31, -HIF1α, -HIF2α and -F4/80 antibodies were purchased from Abcam (Cambridge, MA). Matrigel Basement Membrane Matrix, and Boyden Chambers with and without Matrigel were from BD Biosciences (Bedford, MA).

MiRNA qRT-PCR Detection and Quantification

Hsa-miR-155 and U6 microRNA levels were detected using TaqMan® microRNA Reverse Transcription kit (Applied Biosystem). Briefly, 200 ng of total RNA from each cell line and tumor RNA were used for primer specific reverse transcriptase (RT) in both hsa-miR-155 and U6, and then 2 ul of the RT product was used for subsequent qPCR. The qPCR was performed on ABI HT9600 and data were collected and analyzed using ABI SDS version 2.3. To calculate relative concentration, miR-155 and U6 C_T values for all samples were obtained. A normalized expression for each sample was obtained by dividing C_T of miR-155 by the same sample's U6 CT and designated as ΔC_T. This value is then transformed by performing 2^-(ΔC_T). Furthermore, the ($\Delta\Delta C_T$) method was used in comparing miR-155 expression in immortalized cells to cancer cells or normal breast to cancer tissues according to ABI's protocol.

Plasmids and oligos

Lenti-pMIRNA1-155, pMIRNA1 vector and packaging kit were purchased from System Biosciences (Mountain View, CA). Anti-sense 2'-O-methyl-RNA control and 2'-O-methyl-miR-155 (miR-155 ASO) were custom synthesized from Integrated DNA Technologies (Coralville, Iowa). pMIR-REPORT™ was purchased from Life Technologies Corporation (Carlsbad, CA). Wild type and mutant predicted miR-155 response element (MRE) within VHL-3'UTR was subcloned to pMIR-REPORT™ in SpeI/HindIII sites. The following oligos were used: wild type, F-ctagTTTTTTTTTTTTTTTTTTTTTTTAAAGCTGTTTTTTAATACATTAAATGGTGCTGAGTAAAGGAAA and R-agctTTTCCTTTACTCAGCACCATTTAATGTATTAAAAAACAGCTTTAAAAAAAAAAAAAAAAAAAAAAA; mutant, F-ctagTTTTTTTTTTTTTTTTTTTTTTTAAAGCTGTTTTTTAATAGTAATTATGGTGCTGAGTAAAGGAAA and R-agctTTTCCTTTACTCAGCACCATAATTACTATTAAAAAACAGCTTTAAAAAAAAAAAAAAAAAAAAAAA. In addition, 0.8-kb VHL-3'UTR containing putative miR-155-MRE and its deletion mutant (e.g., lacking miR-155-MRE sequence) were amplified by PCR and the PCR products were cloned to pMIR-REPORT™ in SpeI/HindIII sites. Primers are: F-TCGACTAGTACAGTGGCTCATGCCTGTAATCCC for both constructs, R1-CCGAAGCTTTATTTCCTTTACTCAGCACCAT and R2 –CCGAAGCTTGAACTTCACCGTCTCTTAAGAGCG for the deletion mutant. Myc-tagged Argonaute 2 construct was generously provided by Dr. Gregory J. Hannon (Cold Spring Harbor Laboratory). HA-VHL was from Dr. Michael Ohh (University of Toronto).

Cell culture and tumour specimens

Human breast cancer cell lines were maintained in Dulbecco's modified Eagle's medium (DMEM) containing 10% fetal bovine serum and cultured at 37°C in 5% CO_2. Primary HUVEC were obtained from American Type Culture Collection (Manassas, VA) and maintained in Vascular Cell Basal Medium in the presence and absence of VEGF, EGF, FGF, IGF-1, L-glutamine, heparin sulfate, hydrocortisone, ascorbic acid, and 2% fetal bovine serum and cultured at 37°C in 5% CO_2. Primary human breast cancers and normal

breast specimens were obtained from patients who underwent surgery at H. Lee Moffitt Cancer Center and approved by the institutional review board and in accord with an assurance filed with and approved by the U.S. Department of Health and Human Services. Each cancer specimen contained at least 80% tumour cells, as confirmed by microscopic examination. Tissues were preserved by snap-freeze and stored at −80°C for subsequent protein and RNA extraction with TRIZOL® reagent for RT-qPCR analysis as per instructions.

Endothelial tube formation assay

HUVEC was transfected with pre-miR-155, miR-155-ASO, and control oligos for 12 h and then seeded onto Matrigel coated 96 well plates. Pre-miR-155 and control transfected cells were cultured in a medium without VEGF; whereas miR-155-ASO and control transfected cells were cultured in a medium containing VEGF. After 24 hours incubation, network formation was captured using Zeiss inverted light microscope in combination with AxioVision Software. Quantification of networks was done by measuring total tube length and counting branch points per defined area using ImageJ image data analysis software.

Invasion and migration assay

HUVEC was transfected with pre-miR-155, miR-155-ASO, and control oligos for 12 h and then seeded in upper chamber of Boyden Chambers coated with or without Matrigel in the absence (pre-miR-155-transfected cells) or presence (miR-155-ASO-treated cells). All lower chambers contained normal HUVEC culture medium. After incubation for 48 h, invasion and migration were examined under a Nikon inverted light microscope.

AGO2 RNA co-immunoprecipitation

BT474 cells were transfected with myc-AGO2, pre-miR-155 or control precursor oligos followed by anti-myc/AGO2 RNA immunoprecipitation as previously described [52, 53]. Complementary strand DNA synthesis was done using ImProm-II Reverse Transcription System from Promega (Madison, WI). qRT-PCR was performed using EXPRESS SYBR® GreenER™ qPCR Supermix with Premixed ROX from Life Technologies Corporation (Carlsbad, CA). Primers to detect VHL mRNA: F-ctgcccgtatggctcaactt and R-gtgtgtccctgcatctctgaag; HIF2α mRNA: F-ttgatgtggaaacggatgaa and R-ggaacctgctcttgctgttc and VEGF mRNA: F-gcacccatggcagaagg and R-ctcgattggatggcagtagct.

Target *in vitro* luciferase report and BrdU incorporation assays

Luciferase report assay was performed as described previously [22, 23]. For BrdU incorporation experiment, HUVEC was transfected with pre-miR-155, miR-155-ASO, and control oligos. Following incubation for 36 h, cells were processed for BrdU incorporation according to manufacture's protocol and images captured using Zeiss inverted light microscope and AxioVision Software.

Xenotransplantation and Analysis of Neoangiogenic Blood Vessels, Proliferation and Mitotic Index

Experimental procedures involving animals were reviewed and approved by the Institutional Animal Care and Use committee. Animal care was in accord with institution guidelines. Fifty thousand cells from BT474 which were transfected with various plasmids indicated in the figure legends were injected into mammary fat pad of 6 weeks old female nude mice (Charles River, Wilmington, MA). Tumour growth was monitored every three days by imaging and caliper measurements (LxWxD), until the largest tumour surpassed 1400 mm^3 in size. Tumours were extracted and processed for Western, qRT-PCR, immunohistochemistry, immunofluorescence and histopathological analysis. Neoangiogenic blood vessels and proliferation were evaluated by immunostaining of tumor sections with anti-CD31 and Ki-67. Mitotic indices were determined on H&E-stained sections under microscopy.

Statistical Analysis

Statistical comparisons were based upon unpaired Student's *t* test. Tumour-related death was calculated and follow-up time was determined from the date of diagnosis to the date of tumour-related death or the last follow-up for survivors, and overall survival was estimated with the Kaplan–Meier method. Patients dying from causes other than their cancer were censored at their date of death. The regression analyses were adjusted for tumour stage (I/II and III/IV). These analyses were performed using the SPSS 11.5 Statistical Software (SPSS). Hazard ratios were assessed using the univariate and multivariate Cox proportional hazards models. Clinical variables, including age, stage, grade and tumour histology were adjusted in multivariate Cox proportional hazards model. $P \leq 0.05$ was considered to be statistically significant.

Supplementary Material

Refer to Web version on PubMed Central for supplementary material.

Acknowledgments

FUNDING

This work was supported by grants from the National Institute of Health (CA114343 to TAS, CA115308 to JYD, and CA137041 to JQC) and Florida Bankhead-Coley Cancer Research Program (2BB01 to JQC).

REFERENCES

1. Baeriswyl V, Christofori G. The angiogenic switch in carcinogenesis. Semin Cancer Biol. 2009; 19:329–337. [PubMed: 19482086]
2. Bergers G, Benjamin LE. Tumourigenesis and the angiogenic switch. Nat Rev Cancer. 2003; 3:401–410. [PubMed: 12778130]
3. Bouck N, Stellmach V, Hsu SC. How tumours become angiogenic. Adv Cancer Res. 1996; 69:135–174. [PubMed: 8791681]
4. Folkman J, Watson K, Ingber D, Hanahan D. Induction of angiogenesis during the transition from hyperplasia to neoplasia. Nature. 1989; 339:58–61. [PubMed: 2469964]

5. Folkman J. Role of angiogenesis in tumour growth and metastasis. Semin Oncol. 2002; 29:15–18. [PubMed: 12516034]
6. Hanahan D, Folkman J. Patterns and emerging mechanisms of the angiogenic switch during tumourigenesis. Cell. 1996; 86:353–364. [PubMed: 8756718]
7. Allavena P, Sica A, Solinas G, Porta C, Mantovani A. The inflammatory micro-environment in tumour progression: the role of tumour-associated macrophages. Crit Rev Oncol Hematol. 2008; 66:1–9. [PubMed: 17913510]
8. Balkwill F. Cancer and the chemokine network. Nat Rev Cancer. 2004; 4:540–550. [PubMed: 15229479]
9. Solinas G, Germano G, Mantovani A, Allavena P. Tumour-associated macrophages (TAM) as major players of the cancer-related inflammation. J Leukoc Biol. 2009; 86:1065–1073. [PubMed: 19741157]
10. Folkman J. Angiogenesis in cancer, vascular, rheumatoid and other disease. Nat Med. 1995; 1:27–31. [PubMed: 7584949]
11. Risau W. Mechanisms of angiogenesis. Nature. 1997; 386:671–674. [PubMed: 9109485]
12. Bartel DP. MicroRNAs: target recognition and regulatory functions. Cell. 2009; 136:215–233. [PubMed: 19167326]
13. Cha ST, Chen PS, Johansson G, Chu CY, Wang MY, Jeng YM, et al. MicroRNA-519c suppresses hypoxia-inducible factor-1alpha expression and tumour angiogenesis. Cancer Res. 2010; 70:2675–2685. [PubMed: 20233879]
14. Yamakuchi M, Lotterman CD, Bao C, Hruban RH, Karim B, Mendell JT, et al. P53-induced microRNA-107 inhibits HIF-1 and tumour angiogenesis. Proc Natl Acad Sci USA. 2010; 107:6334–6339. [PubMed: 20308559]
15. Fang L, Deng Z, Shatseva T, Yang J, Peng C, Du WW, et al. MicroRNA miR-93 promotes tumour growth and angiogenesis by targeting integrin-beta8. Oncogene. 2011; 30:806–821. [PubMed: 20956944]
16. Eis PS, Tam W, Sun L, Chadburn A, Li Z, Gomez MF, et al. Accumulation of miR-155 and BIC RNA in human B cell lymphomas. Proc Natl Acad Sci USA. 2005; 102:3627–3632. [PubMed: 15738415]
17. Iorio MV, Ferracin M, Liu CG, Veronese A, Spizzo R, Sabbioni S, et al. MicroRNA gene expression deregulation in human breast cancer. Cancer Res. 2005; 65:7065–7070. [PubMed: 16103053]
18. Kluiver J, Poppema S, de Jong D, Blokzijl T, Harms G, Jacobs S, et al. BIC and miR-155 are highly expressed in Hodgkin, primary mediastinal and diffuse large B cell lymphomas. J Pathol. 2005; 207:243–249. [PubMed: 16041695]
19. Volinia S, Calin GA, Liu CG, Ambs S, Cimmino A, Petrocca F, et al. A microRNA expression signature of human solid tumours defines cancer gene targets. Proc Natl Acad Sci USA. 2006; 103:2257–2261. [PubMed: 16461460]
20. Yanaihara N, Caplen N, Bowman E, Seike M, Kumamoto K, Yi M, et al. Unique microRNA molecular profiles in lung cancer diagnosis and prognosis. Cancer Cell. 2006; 9:189–198. [PubMed: 16530703]
21. Jiang S, Zhang HW, Lu MH, He XH, Li Y, Gu H, et al. MicroRNA-155 functions as an OncomiR in breast cancer by targeting the suppressor of cytokine signaling 1 gene. Cancer Res. 2010; 70:3119–3127. [PubMed: 20354188]
22. Kong W, Yang H, He L, Zhao JJ, Coppola D, Dalton WS, et al. MicroRNA-155 is regulated by the transforming growth factor beta/Smad pathway and contributes to epithelial cell plasticity by targeting RhoA. Mol Cell Biol. 2008; 28:6773–6784. [PubMed: 18794355]
23. Kong W, He L, Coppola M, Guo J, Esposito NN, Coppola D, et al. MicroRNA-155 regulates cell survival, growth, and chemosensitivity by targeting FOXO3a in breast cancer. J Biol Chem. 2010; 285:17869–17879. [PubMed: 20371610]
24. O'Connell RM, Taganov KD, Boldin MP, Cheng G, Baltimore D. MicroRNA-155 is induced during the macrophage inflammatory response. Proc Natl Acad Sci USA. 2007; 104:1604–1609. [PubMed: 17242365]

25. Pedersen IM, Otero D, Kao E, Miletic AV, Hother C, Ralfkiaer E, et al. Onco-miR-155 targets SHIP1 to promote TNFalpha-dependent growth of B cell lymphomas. EMBO Mol Med. 2009; 1:288–295. [PubMed: 19890474]
26. Thai TH, Calado DP, Casola S, Ansel KM, Xiao C, Xue Y, et al. Regulation of the germinal center response by microRNA-155. Science. 2007; 316:604–608. [PubMed: 17463289]
27. Tili E, Michaille JJ, Cimino A, Costinean S, Dumitru CD, Adair B, et al. Modulation of miR-155 and miR-125b levels following lipopolysaccharide/TNF-alpha stimulation and their possible roles in regulating the response to endotoxin shock. J Immunol. 2007; 179:5082–5089. [PubMed: 17911593]
28. Tili E, Michaille JJ, Wernicke D, Alder H, Costinean S, Volinia S, et al. Mutator activity induced by microRNA-155 (miR-155) links inflammation and cancer. Proc Natl Acad Sci USA. 2011; 108:4908–4913. [PubMed: 21383199]
29. Vigorito E, Perks KL, Abreu-Goodger C, Bunting S, Xiang Z, Kohlhaas S, et al. microRNA-155 regulates the generation of immunoglobulin class-switched plasma cells. Immunity. 2007; 27:847–859. [PubMed: 18055230]
30. Babar IA, Czochor J, Steinmetz A, Weidhaas JB, Glazer PM, Slack FJ. Inhibition of hypoxia-induced miR-155 radiosensitizes hypoxic lung cancer cells. Cancer Biol Ther. 2011; 12:908–914. [PubMed: 22027557]
31. Suarez Y, Fernandez-Hernando C, Yu J, Gerber SA, Harrison KD, Pober JS, et al. Dicer-dependent endothelial microRNAs are necessary for postnatal angiogenesis. Proc Natl Acad Sci USA. 2008; 105:14082–14087. [PubMed: 18779589]
32. Coultas L, Chawengsaksophak K, Rossant J. Endothelial cells and VEGF in vascular development. Nature. 2005; 438:937–945. [PubMed: 16355211]
33. Jain RK. Molecular regulation of vessel maturation. Nat Med. 2003; 9:685–693. [PubMed: 12778167]
34. Kaelin WG Jr. The von Hippel-Lindau tumour suppressor protein: O2 sensing and cancer. Nat Rev Cancer. 2008; 8:865–873. [PubMed: 18923434]
35. Andorfer CA, Necela BM, Thompson EA, Perez EA. MicroRNA signatures: clinical biomarkers for the diagnosis and treatment of breast cancer. Trends Mol Med. 2011; 17:313–319. [PubMed: 21376668]
36. Suárez Y, Sessa WC. MicroRNAs as novel regulators of angiogenesis. Circ Res. 2009; 104:442–454. [PubMed: 19246688]
37. Kim WY, Kaelin WG. Role of VHL gene mutation in human cancer. J Clin Oncol. 2004; 22:4991–5004. [PubMed: 15611513]
38. Zia MK, Rmali KA, Watkins G, Mansel RE, Jiang WG. The expression of the von Hippel-Lindau gene product and its impact on invasiveness of human breast cancer cells. Int J Mol Med. 2007; 20:605–611. [PubMed: 17786294]
39. Greer SN, Metcalf JL, Wang Y, Ohh M. The updated biology of hypoxia-inducible factor. EMBO J. 2012; 3:2448–2460. [PubMed: 22562152]
40. Krishnamachary B, Penet MF, Nimmagadda S, Mironchik Y, Raman V, Solaiyappan M, Semenza GL, Pomper MG, Bhujwalla ZM. Hypoxia regulates CD44 and its variant isoforms through HIF-1α in triple negative breast cancer. PLoS One. 2012; 7:e44078. [PubMed: 22937154]
41. Montagner M, Enzo E, Forcato M, Zanconato F, Parenti A, Rampazzo E, Basso G, Leo G, Rosato A, Bicciato S, Cordenonsi M, Piccolo S. SHARP1 suppresses breast cancer metastasis by promoting degradation of hypoxia-inducible factors. Nature. 2012; 487:380–384. [PubMed: 22801492]
42. Li M, Kim WY. Two sides to every story: the HIF-dependent and HIF-independent functions of pVHL. J Cell Mol Med. 2011; 15:187–195. [PubMed: 21155973]
43. Albini A, Tosetti F, Benelli R, Noonan DM. Tumour inflammatory angiogenesis and its chemoprevention. Cancer Res. 2005; 65:10637–10641. [PubMed: 16322203]
44. Bergers G, Hanahan D, Coussens LM. Angiogenesis and apoptosis are cellular parameters of neoplastic progression in transgenic mouse models of tumourigenesis. Int J Dev Biol. 1998; 42:995–1002. [PubMed: 9853830]

45. Skobe M, Rockwell P, Goldstein N, Vosseler S, Fusenig NE. Halting angiogenesis suppresses carcinoma cell invasion. Nat Med. 1997; 3:1222–1227. [PubMed: 9359696]

46. Coussens LM, Werb Z. Inflammation and cancer. Nature. 2002; 420:860–867. [PubMed: 12490959]

47. Luo JL, Maeda S, Hsu LC, Yagita H, Karin M. Inhibition of NF-kappaB in cancer cells converts inflammation- induced tumour growth mediated by TNFalpha to TRAIL-mediated tumour regression. Cancer Cell. 2004; 6:297–305. [PubMed: 15380520]

48. Ono M. Molecular links between tumour angiogenesis and inflammation: inflammatory stimuli of macrophages and cancer cells as targets for therapeutic strategy. Cancer Sci. 2008; 99:1501–1506. [PubMed: 18754859]

49. Chang S, Wang RH, Akagi K, Kim KA, Martin BK, Cavallone L, et al. Tumour suppressor BRCA1 epigenetically controls oncogenic microRNA-155. Nat Med. 2011; 17:1275–1282. [PubMed: 21946536]

50. Foulkes WD, Stefansson IM, Chappuis PO, Begin LR, Goffin JR, Wong N, et al. Germline BRCA1 mutations and a basal epithelial phenotype in breast cancer. J Natl Cancer Inst. 2003; 95:1482–1485. [PubMed: 14519755]

51. Lakhani SR, Reis-Filho JS, Fulford L, Penault-Llorca F, van der Vijver M, Parry S, et al. Prediction of BRCA1 status in patients with breast cancer using estrogen receptor and basal phenotype. Clin Cancer Res. 2005; 11:5175–5180. [PubMed: 16033833]

52. Karginov FV, Conaco C, Xuan Z, Schmidt BH, Parker JS, Mandel G, et al. A biochemical approach to identifying microRNA targets. Proc Natl Acad Sci USA. 2007; 104:19291–19296. [PubMed: 18042700]

53. Keene JD, Komisarow JM, Friedersdorf MB. RIP-Chip: the isolation and identification of mRNAs, microRNAs and protein components of ribonucleoprotein complexes from cell extracts. Nat Protoc. 2006; 1:302–307. [PubMed: 17406249]

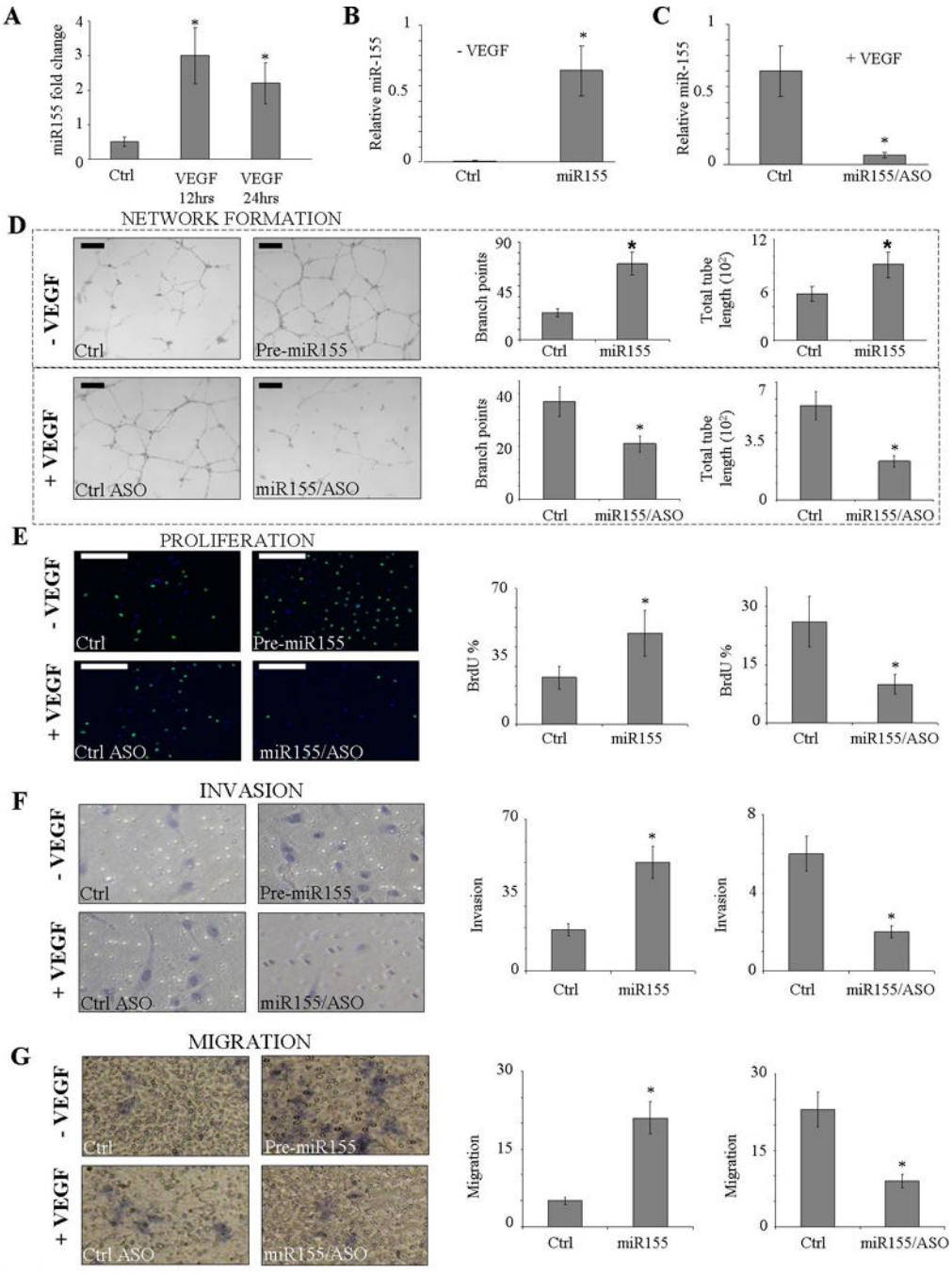

Figure 1. Expression of miR-155 induces and knockdown of miR-155 represses *in vitro* angiogenesis

(**a** and **b**) HUVECs were transfected with indicated oligos and then cultured in the absence or presence of VEGF for 48 h. (**c**) HUVECs were treated with VEGF for indicated times and then subjected to qRT-PCR analysis of miR-155 level. The HUVECs were examined for: (**d**) endothelial network formation (Scale bar, 250 μM) and branch points and total tube length quantification, (**e**) proliferation (Scale bar, 250 μM) by BrdU incorporation, (**f**) invasion (100 × magnification) and (**g**) migration (100X magnification). Images

representative of experiments was performed in triplicates for 2 times. (Mean ± SEM, n=6). Asterisk indicates $p<0.05$.

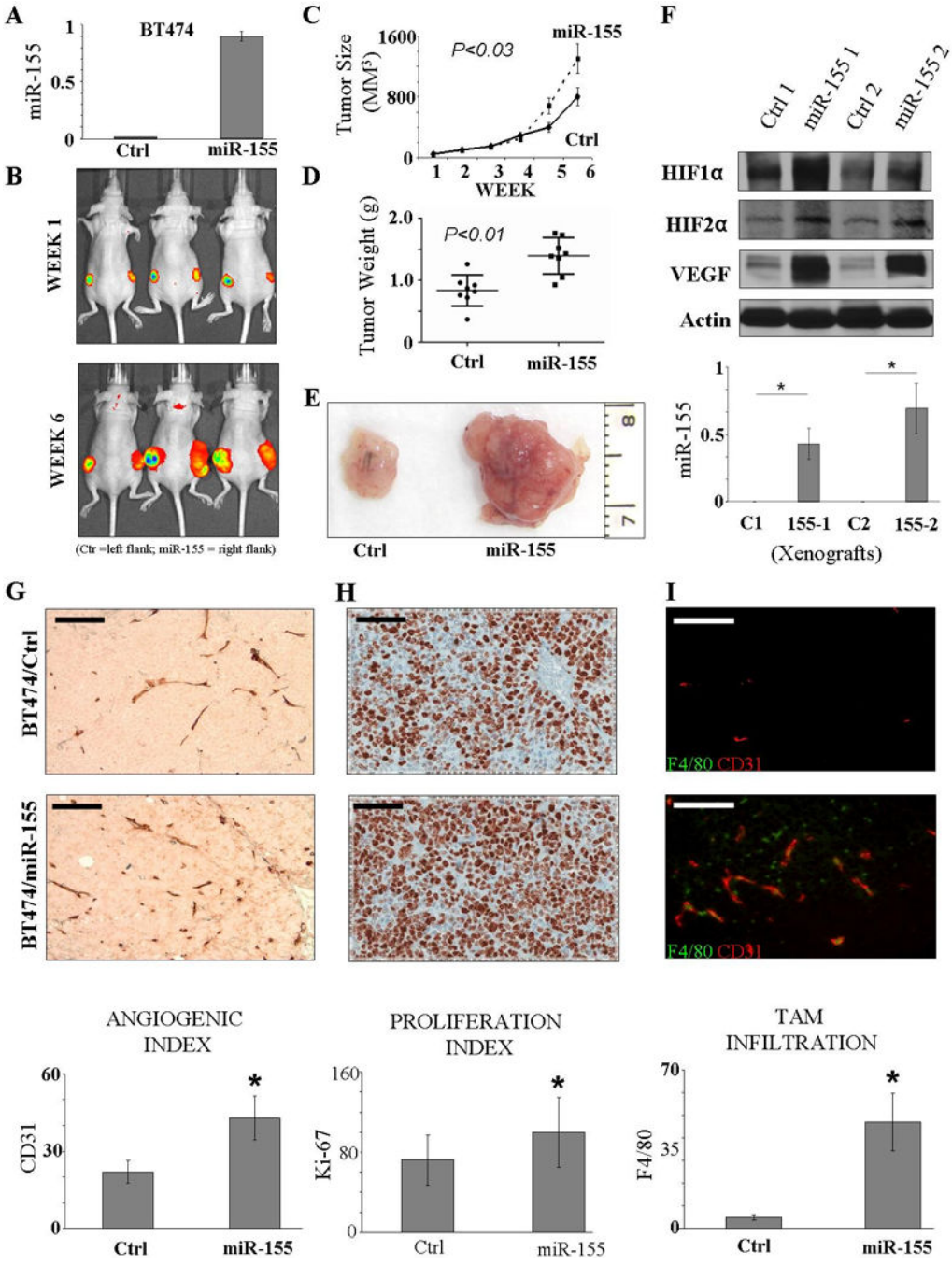

Figure 2. The effects of miR-155 on *in vivo* angiogenesis

(**a**) BT474 cells were stably infected with lentivirus expressing miR-155 (BT474/miR-155) and control vector (BT474/Ctrl) and then subjected to qRT-PCR analysis. (**b**) Representative images of bioluminescent BT474/Ctrl and BT474/miR-155 xenograft tumours captured on the IVIS Imaging system on day 5 (top) of transplantation and experimental endpoint (bottom). (**c** and **d**) MiR-155 induces tumour growth. Tumour growth were monitored for 6 weeks and tumour weight was calculated at the completion of experiment (Mean ± SEM, n=8). (**e**) BT474/miR-155 tumour presents more blood vessels. Representative tumours from

BT474/Ctrl and BT474/miR-155 xenografts. (**f**) MiR-155 up-regulates HIF1α, HIF2α and VEGF. Western blot analysis of representative xenograft tumours with indicated antibodies (upper panels). Expression of miR-155 in these tumours was evaluated by qRT-PCR (bottom panel). (**g**)-(**i**) MiR-155 induces angiogenesis, proliferation and tumour associated macrophage (TAM) infiltration. Panels g and h are immunohistochemical staining with CD31 and Ki-67 antibodies (upper). Bottom panels show quantification of neoangiogenic blood vessels and positive Ki-67 cells. Panel i is co-immunofluorescence staining with antibodies against F4/80 (green) and CD31 (red). TAM infiltration was determined/quantified by average of F4/80 positive cells. Asterisk indicates $p<0.05$.

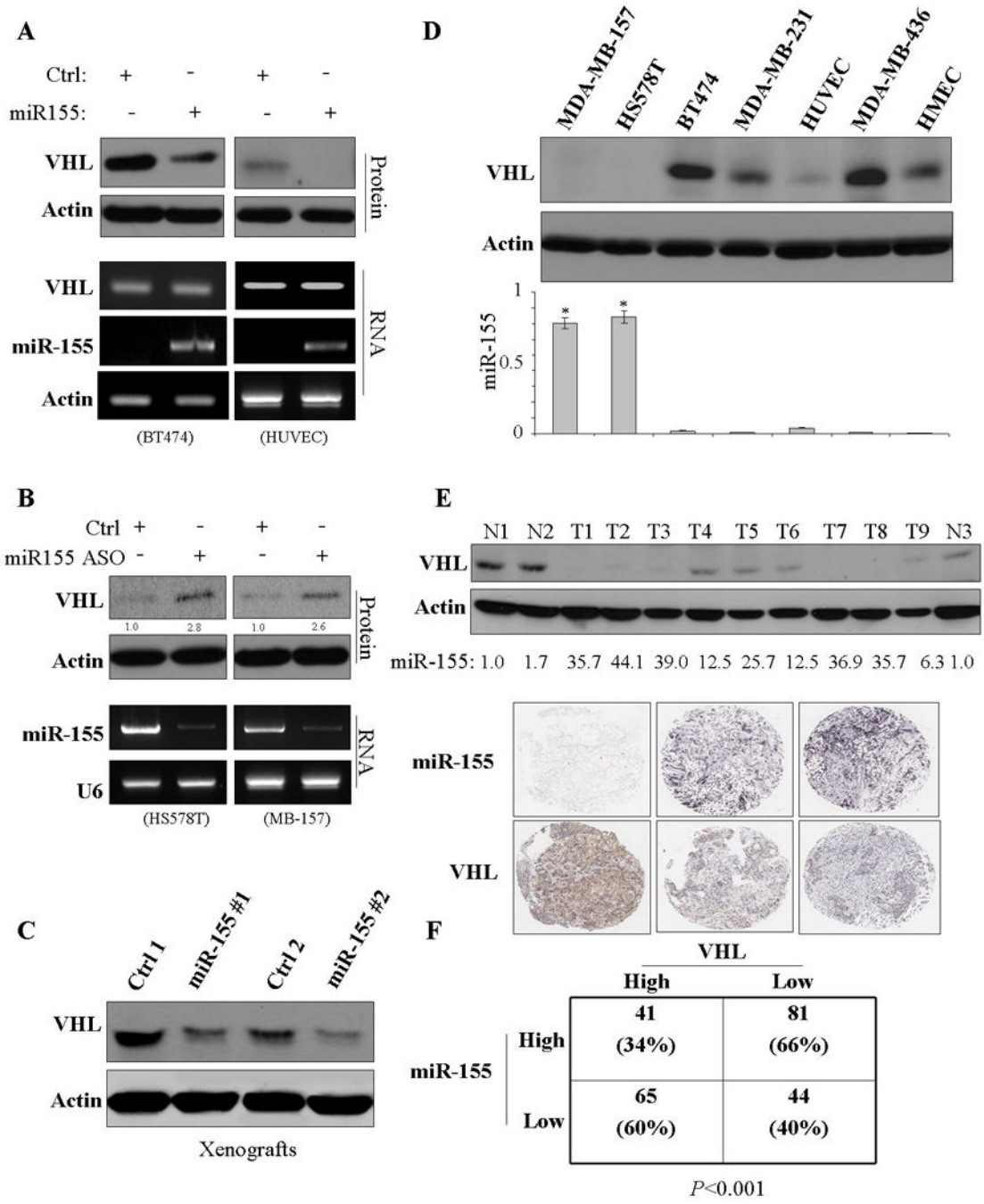

Figure 3. MiR-155 regulates VHL at protein level

(**a**) Reduction of VHL protein by ectopic cxpression of miR-155. MiR-155-low cells, BT474 and HUVEC, were transfected with pre-miR-155 and control oligos and then subjected to immunoblot and semi-quantitative RT-PCR analyses. (**b**) VHL is increased by knockdown of miR-155. MiR-155-high cell lines, HS578T, and MDA-MB-157, were treated with anti-miR-155 (ASO) and control oligo and analyzed for VHL protein levels. (**c**) downregulation of VHL by miR-155 *in vivo*. Western blot analysis of xenograft tumours with antibodies against VHL (top) and actin (bottom). (**d** and **e**) VHL levels are negatively correlated with

miR-155 expression in breast cancer. Breast cancer cell lines (d) and primary tumours (e) were analyzed for expression of VHL and miR-155 by immunoblot with indicated antibodies (upper panels), qRT-PCR (middle) and LNA-ISH (bottom). (**f**) Chi-square test analysis of miR-155 and VHL expression in 82 breast cancer specimens examined. The inverse correlation is significant ($p = 0.042$).

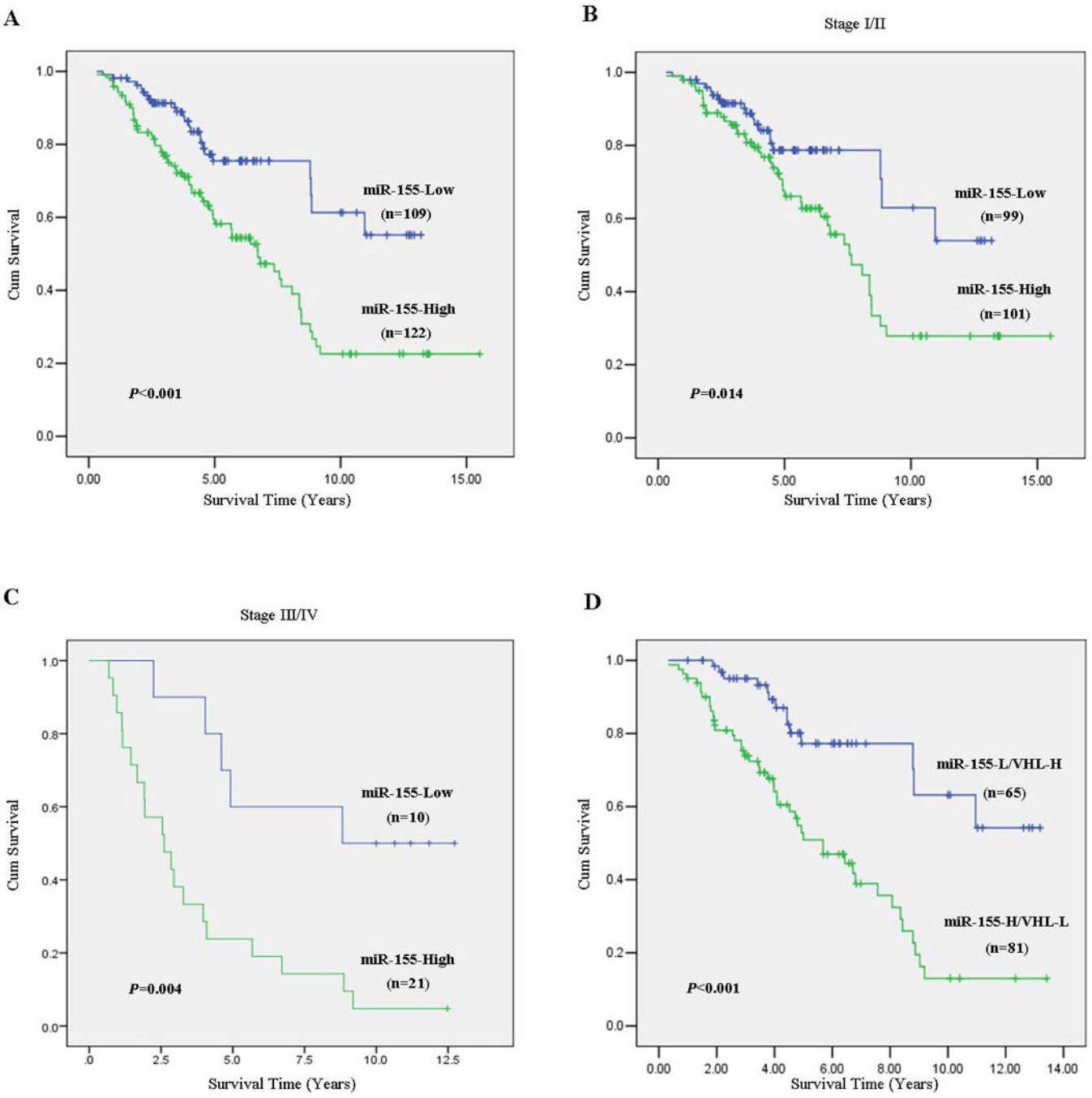

Figure 4. MiR-155 expression associates with poor survival in breast cancer

(**a**) MiR-155 low and high expression cut-point that best associates with patient 10 year survival within the cancer subpopulation was determined by X-Tile algorithm, where a division at 90.1412 yield a statistically significant difference in 10 year overall survival in original data set and (**b**) software randomly derived validation set. (**c**) Overall survival (OS) in patients with high levels of mR-155 (n = 61) versus the remaining patients (n = 21) was plotted by the Kaplan-Meier method. Statistical comparison of survival between groups with the log-rank statistic analysis suggests that patients whose tumours express elevated levels

of miR-155 had poor survival compared to those with low levels of miR-155 ($P = 0.008$). (**d**) OS was also analyzed in patients with early stage and (**e**) late stage breast tumours expressing high versus low levels of miR-155 as well as (**f**) combination of miR-155 and VHL expression.

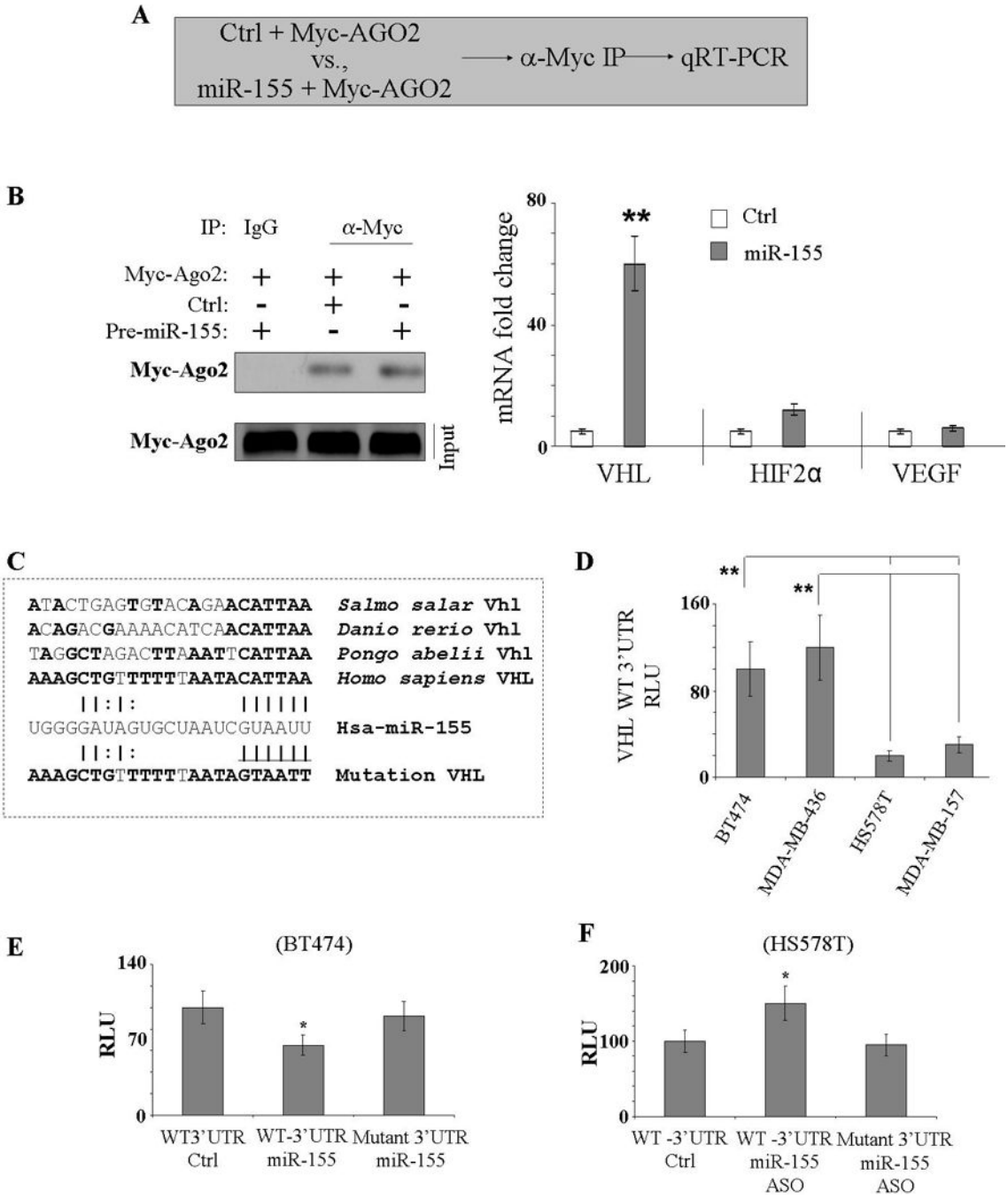

Figure 5. Direct interaction of miR-155 with VHL

(**a**) Schematic procedures of AGO2 RNA immunoprecipitation. (**b**) VHL is enriched in miR-155/AGO2/RISC complex. BT474 cells were transfected with myc-AGO2 together with or without pre-miR-155 and then immunoprecipitated with anti-myc antibody (left panel). The immunoprecipitates (e.g., miR-155/AGO2/RISC complex) were subjected to qRT-PCR analysis of VHL, HIF2α and VEGF (right). (**c**) RNA22 miRNA target detection analysis reveals a non canonical, but conserved miR-155 response element within 3'UTR of VHL mRNA. (**d**)-(**f**) Luciferase reporter assay. Indicated cells were transfected with

indicated plasmids and oligo as well as β-galactosidase. After incubation for 48 h, cells subjected to luciferase assay. Luciferase activity was normalized with β-galactosidase. Relative luciferase activities are presented. Data represent three independent experiments in triplicate. Single and double asterisks indicate $p < 0.05$ and $p < 0.005$, respectively.

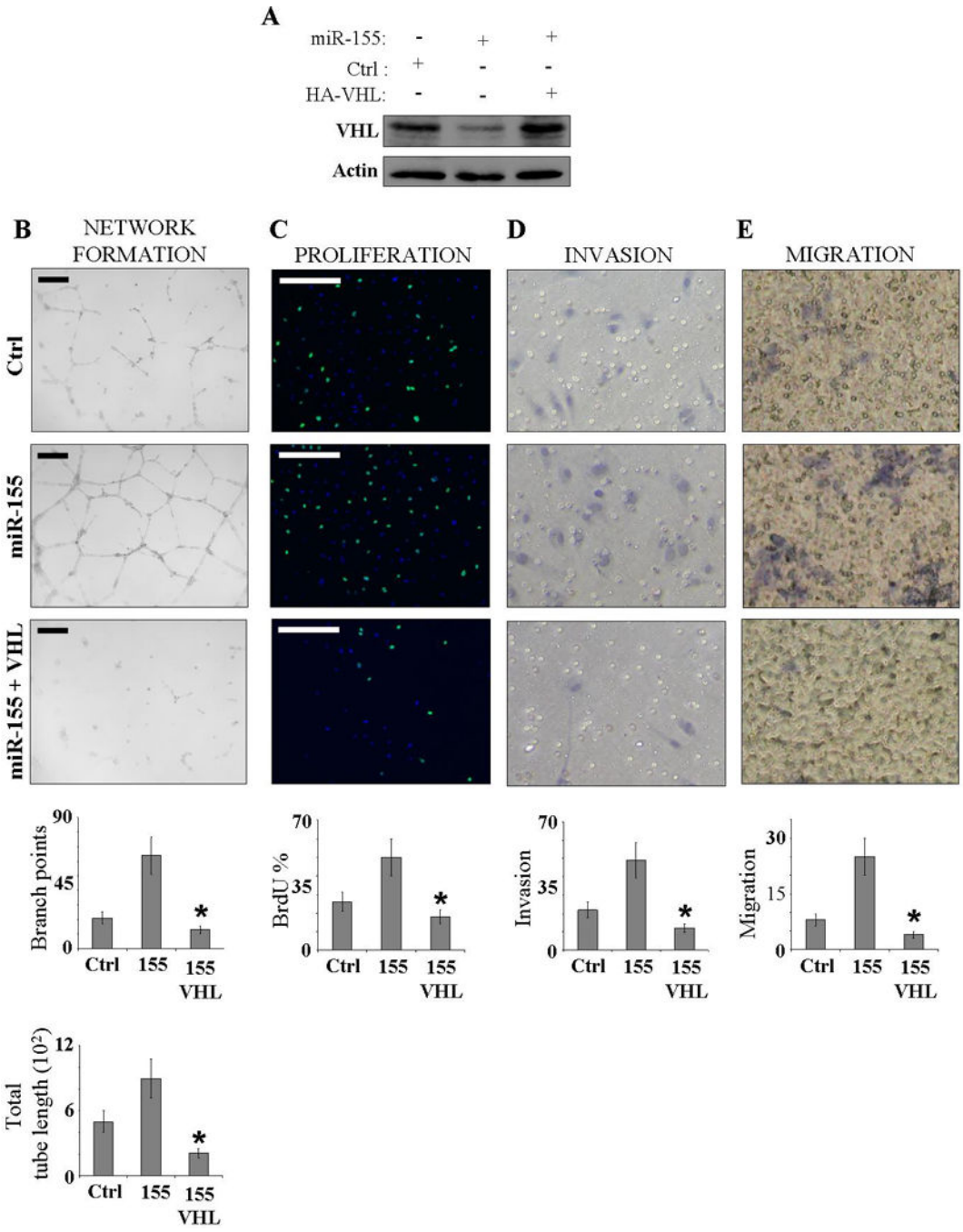

Figure 6. Transfection of VHL cDNA lacking 3'-UTR overrides *miR-155* effects on *in vitro* angiogenesis

(**a**) Western blot analysis of HUVEC transfected with indicated plasmids. The transfected cells were assayed for endothelial network formation (Scale bar, 250 μM) with branch points, and total tube length quantitation (**b**), proliferation (**c**) invasion (**d**) and migration (**e**). Bottom panels show the quantification of 3 experiments in triplicates. Asterisks indicate $p < 0.05$.

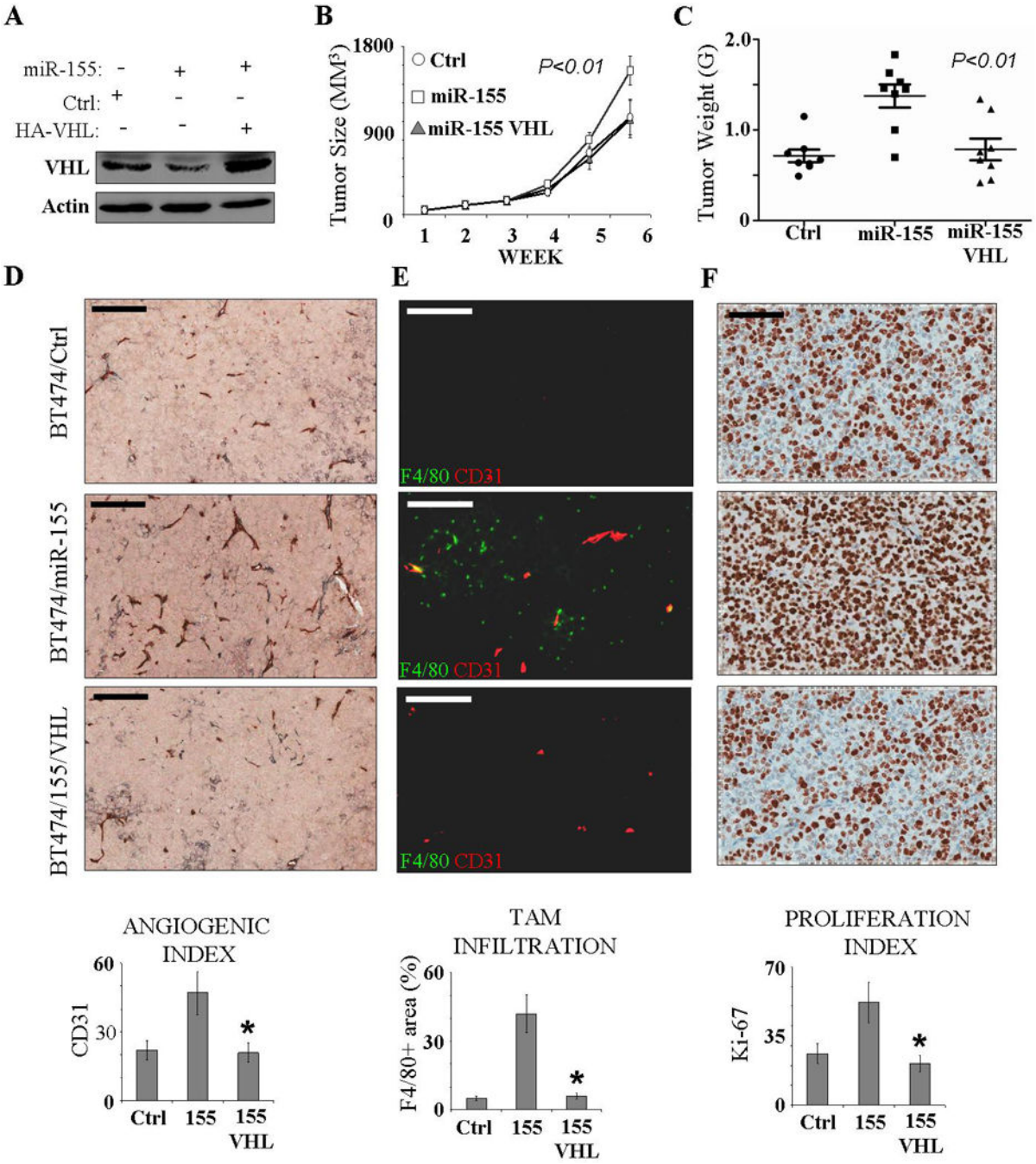

Figure 7. VHL reconstitution inhibits miR-155-induced *in vivo* angiogenesis

(**a**) BT474 cells were transfected with indicated plasmids and then immunoblotted with indicated antibodies. The cells were injected to mammary fat pad and examined for tumour growth (**b**) and tumour weight (Mean ± SEM, n=8; **c**). The tumours were sectioned and evaluated for angiogenic index (**d**), TAM infiltration (**e**) and proliferation index (**f**).

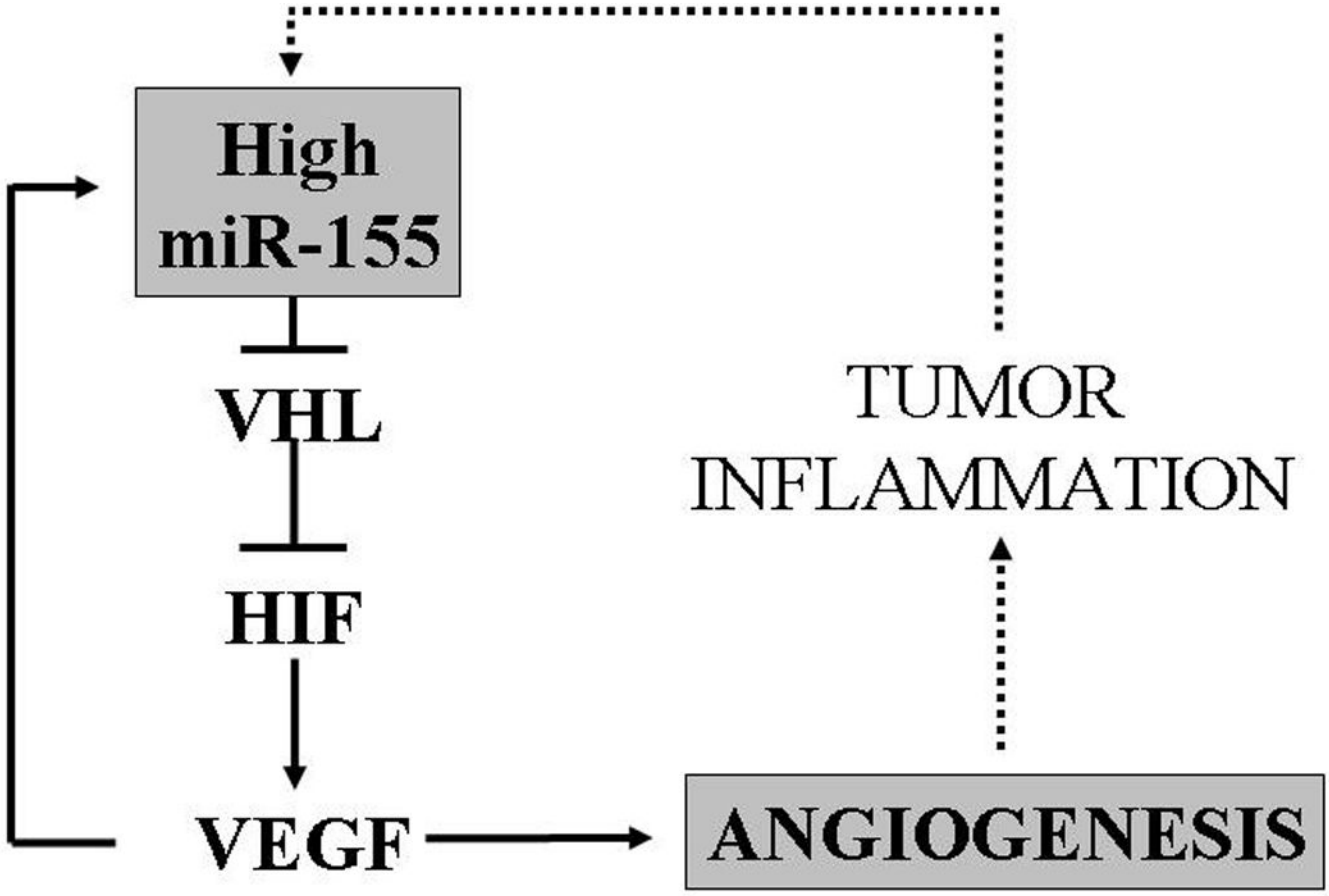

Figure 8.
Diagram depicting the miR-155 regulation of angiogenesis

Table 1

MiR-155 expression in clinical and pathological characteristics

Characteristics	N	miR-155 Low/No	miR-155 High/Mod	*P* value
Age				0.229
≤51	99	50	49	
>51	132	59	73	
Stage				0.054
I/II	200	99	101	
III/IV	31	10	21	
Grade				0.018
I/II	62	36	26	
III	160	66	94	
Node				<0.001
Negative (<10)	173	91	82	
Positive (≥10)	39	8	31	
ER-/PR-/HER2- (Triple Negative)				<0.001
No	152*	107	45	
Yes	36*	7	29	

Analysis with $X2$ test.

*Cases with complete ER/PR/HER2 status.

Table 2

Ten-year survival analysis of patients with breast tumor

	Univariate Analysis		Multivariate Analysis	
Variable	**HR* (95% CI†)**	***P* value**	**HR (95% CI)**	***P* value**
Age				
≤51 years vs. >51	0.995 (0.664–1.539)	**0.984**	1.259 (0.807–1.964)	**0.311**
Histology				
Ductal vs. other types	2.325 (1.494–3.619)	<**0.001**	1.735 (1.096–2.745)	**0.019**
Stage				
Early (I/II) vs. Late (III/IV)	2.354 (1.463–3.786)	<**0.001**	2.135 (1.303–3.498)	**0.003**
Grade				
Low (I/II) vs. High (III)	1.653 (0.988–2.768)	**0.056**	1.420 (0.836–2.412)	**0.194**
miR-155				
≤90 vs. >90	2.408 (1.491–3.888)	<**0.001**	2.377 (1.461–3.866)	<**0.001**

*HR: Hazard Ratio

†CI: Confidence Ratio